Polyaniline/Carbon Black Composite as Pt Electrocatalyst Supports for Methanol Oxidation: Synthesis and Characterization

Bo Qu,[1,2] Yiting Xu,[1] Yuanming Deng,[1] Xiaoliang Peng,[1] Jiangfeng Chen,[1] Lizong Dai[1]

[1]*State Key Laboratory for Physical Chemistry of Solid Surfaces and Department of Materials Science and Engineering, College of Materials, Xiamen University, Xiamen, Fujian 361005, People's Republic of China*
[2]*School of Chemical and Biological Science, Quanzhou Normal University, Quanzhou, Fujian 362000, People's Republic of China*

Received 25 June 2008; accepted 17 February 2010
DOI 10.1002/app.32282
Published online 10 June 2010 in Wiley InterScience (www.interscience.wiley.com).

ABSTRACT: Core/shell composites of polyaniline (PANI) and Vulcan XC-72 Carbon (VC), in which the carbon represents the core and PANI forms the shell, were synthesized by *in situ* chemical oxidation polymerization. Platinum (Pt) particles were then deposited on the PANI/VC composites by chemical reduction method. The highest conductivity is obtained when a mass ratio of PANI/VC equals to 0.28, as proved by Fourier transform infrared spectra. And it is also proved that there are some reactions happened between PANI and VC. Scanning electron microscope, transmission electron microscope, and X-ray diffraction measurements were performed to analyze their structure and surface morphology. It has been observed that the Pt particles are smaller in size and more uniformly distributed on these composite supports than on pure VC supports, considered as a reference. Methanol oxidation performed on the electrode modified by such a composite catalyst has been measured by cyclic voltammogram focusing on the attenuation of methanol oxidation current after 200 cycles. The attenuation degree for the composite catalyst is only one-third of the one measured for a simple Pt/VC catalyst. It is proved that the composite catalyst better resist carbon monoxide poisoning in comparison with the Pt/VC catalyst, which may be due to the synergetic effects between the composite support and the Pt catalyst. © 2010 Wiley Periodicals, Inc. J Appl Polym Sci 118: 2034–2042, 2010

Key words: polyaniline carbon black; *in situ* polymerization; methanol electrocatalytic oxidation; CO antipoisoning

INTRODUCTION

Thanks to the progresses gradually achieved by the fundamental research about methanol oxidation,[1,2] the direct methanol fuel cell (DMFC) will soon become attractive in comparison with the hydrogen fuel cell. Over the past several decades, researchers identified platinum (Pt) as the most suitable catalyst in DMFC systems. However, it is well known that some intermediate products of the reaction are strongly adsorbed at the electrode surface, acting as a poison (e.g., adsorbed carbon monoxide, CO_{ads}) and leading to a loss of the electrocatalytic activity of the electrode. To increase the antipoisoning ability of Pt catalysts, many ways have been reported in the literature. One way is represented by Pt alloy technologies, including binary and ternary alloy, such as Pt-Ru,[3–5] and Pt-Ru-M (M = Mo,[6] W,[7] Os[8]). However, the possibility of preparing composite catalysts with a conducting polymer and an adequate carbon support is another attractive way.

Mesocarbon microbeads,[9] carbon nanotubes,[10–12] graphite carbon nanofibres,[13] mesoporous carbon materials,[14,15] hollow-core mesoporous-shell carbon capsules,[16] and carbon nanocoils[17] are some of the most popular carbon materials, which could be used as catalyst supports. In particular, commercial carbon black Vulcan XC-72 carbon (VC), whose specific surface is close to 250 m^2/g, is commonly used as a catalyst support in DMFC. However, the Pt catalytic efficiency and its service life in traditional platinized VC catalysts are not ideal, essentially due to the fact

Correspondence to: Y. Xu (xyting@xmu.edu.cn) or L. Dai (lzdai@xmu.edu.cn).

Contract grant sponsor: Research Fund for the Doctoral Program of Higher Education; contract grant number: 20070384047.
Contract grant sponsor: Natural Science Fund of Fujian Province of China; contract grant numbers: E0310003, E0610029.
Contract grant sponsor: Scientific and Technical Project of Fujian Province of China; contract grant numbers: 2006I0026, 2007F3088.
Contract grant sponsor: Scientific and Technical Project of Xiamen City; contract grant number: 3502Z20055020.
Contract grant sponsor: Technical Innovative Program of Xiamen university; contract grant number: XDKJCX20041010.

that carbon materials have low gas permeability and proton conductivity.[18] In recent years, more and more researchers paid attention to the possibility of developing new catalyst supports by using conducting polymers, to improve the performance of fuel cells and to reduce their cost.[19] Polyaniline (PANI) is a widely used conducting polymer, relatively easy to prepare and having a good electrical conductivity, associated to a remarkable environmental stability. PANI electronic properties can be reversibly controlled both by doping/dedoping and by protonation processes, in which its emeralding base and emeraldine salt forms can be interchanged.[20] For such reasons, the use of PANI as a support for DMFC catalyst is becoming one of the most popular research topics.[21–24] The porous structure of this conducting polymer is helpful to build three-dimensionally dispersed Pt systems. In the literature, there are comprehensive reports about conducting polymers with high antipoisoning ability.[25–27] These conducting polymers can accelerate methanol oxidation to carbon dioxide (CO_2), reducing the formation of CO_{ads} toxic intermediates. The catalysts based on PANI membrane electrodes were in most cases prepared by electrochemical polymerization, followed by the electrodeposition of Pt particles. However, the lower conductivity and reduced stability during catalyst processing of conducting polymer supports in comparison with traditional carbon supports still represent a problem to be solved.[28]

Along with the development of composite materials, more and more attention has been paid to conducting polymers and carbon composites.[29,30] In this study, we prepared core-shell PANI/VC composite structures by *in situ* chemical polymerization, in which the core is composed of VC and the shell is made of conducting polymer, followed by the deposition of Pt particles by a chemical deposit method, with the aim of improving the CO antipoisoning ability and catalytic efficiency of the Pt catalyst. The purpose of this article is to confirm the effects of different catalyst supports on the morphology and performances of Pt-loading catalyst, therefore, a fixed Pt percent was chosen and discussed.

EXPERIMENTAL

Materials

VC was purchased from Cabot, USA. Aniline monomer (ANI, Shanghai Chemical Works, China) (99% purity, Aldrich) was distilled under reduced pressure and stored at low temperature before use. Ammonium persulfate (APS), sodium borohydride ($NaBH_4$), hexachloroplatinic acid (H_6PtCl_6), concentrated sulfuric acid (H_2SO_4, 98%), nitric acid (HNO_3, 60%), and any other organic solvents needed are of analytical grade and used without further purification. In this work, only deionized water was used. 5% Polytetrafluoroethylene (PTFE) emulsion was purchased and used as received.

Synthesis of PANI/VC composites

VC particles were pretreated by boiling in 4 mol/L HNO_3 solution for 4 h, then washed with deionized water until pH = 7. A certain amount of treated VC was dispersed in 1 mol/L H_2SO_4 solutions by ultrasonic over 1 h, then the solution was transferred to magnetic stirring apparatus equipped with an ice-bath. ANI monomer was then added to the above suspension of carbon nanoparticles. 20 mL of 1 mol/L H_2SO_4 solution containing APS (molar ratio ANI/APS = 1) was slowly added to the suspension keeping constant magnetic stirring, at a reaction temperature of 0–5°C for 15 min. After further 6 h stirring, the resulting green suspension was filtered and rinsed several times with distilled water and methanol until filter became neutral and colorless. The obtained powder was dried in a vacuum oven at 60°C for 24 h.

Preparation of Pt/PANI/VC catalysts

0.1 g of the composite material obtained as previously described were suspended in 50 mL of an acetic acid buffer solution (pH = 4) and the following suspension was ultrasonically stirred for 30 min. Thereafter, 1.65 mL of H_6PtCl_6 solution with a concentration of 0.077 mol/L was added to the suspension and magnetic stirred for 2 h. An excessive amount of $NaBH_4$ solution was added to the suspension. Afterward, the mixture was heated to 80°C and kept to such constant temperature for 1 h. The Pt/PANI/VC catalyst was finally filtered and washed with an excess of deionized water, then dried at 70°C under vacuum for 24 h.

The reference Pt/VC catalyst was prepared with the same route by rather using VC as the supporting material.

Preparation of catalyst electrodes

First of all, the glassy carbon (GC) electrode (d = 5 mm) was polished, then ultrasonic washed in deionized water and 5 mol/L HNO_3 solution for 5 min, respectively. Finally, the GC electrode was rinsed by water. An amount of the previously prepared catalyst powder was mixed with isopropanol, 5% PTFE emulsion, and deionized water in an ultrasonic oscillator to obtain a homogeneous ink-like solution. The electrode modified by the catalyst was then prepared by pipetting the solution onto the surface of

the GC electrode, followed by drying under infrared light.

Characterization

The morphology of the supporting material and of the composite catalyst was observed by scanning electron microscope (SEM) and transmission electron microscope (TEM), performed on a LEO-1530 and a F30 TEM microscope, respectively.

X-ray Diffraction (XRD) measurements were obtained on a Panalytical X'Pert diffractometer using a Cu $K\alpha_1$ X-ray source operating at 40 kV and 30 mA, at a scan rate of 0.1°/min.

Fourier Transform Infrared (FTIR) Spectra were recorded by a Nicolet Avatar 360 fourier infrared spectrophotometer with the KBr pellet technique.

Elementary analysis was performed on a EA1110-CE instrument to identify the components of the composite support.

Measurements of the electric conductivity were performed by the four-points technique (Suzhou Baishen SZ 82) on sample pellets (1.5 cm diameter) compressed at room temperature by 100 MPa for 5 min.

Electrochemical characterizations of the electrode modified by the catalyst were performed on a EG&G 263 electrochemical working station using a standard three-electrode cell. A GC disk covering the catalyst was used as the working electrode. A Pt foil having a surface of 0.5 cm^2 served as the counter electrode. A saturated calomel electrode was used as the reference electrode. Cyclic Voltammogram (CV) was recorded from 0 to 1.0 V at a scan rate of 50 mV/s.

RESULTS AND DISCUSSION

Effect of the PANI/VC molar ratio on the composites

PANI/VC composites used as a support for the catalyst need to have a high specific surface and a good conductivity. Ensuring the optimum PANI/VC ratio is the key factor to prepare a suitable composite support. Too much PANI will decrease the global conductivity of the composite, whereas too little PANI does not justify the use of a conducting polymer, because the main aim is to improve the antipoisoning ability of the catalyst and such properties require a minimum amount of polymer. Unlike traditional composites, in which carbon particles act as a filler in a polymer matrix,[31] we rather used carbon moieties as the matrix material (core) and the polymer as its modifier (shell). The relationship between the PANI/VC mass ratio (effectively found in the composite material) and the feeding ANI/VC ratio (initially introduced in the reacting system) is shown in Table I. By means of elementary analysis, we calculated the actual PANI/VC mass ratio in the obtained composite support. The value of the PANI/VC mass ratio is lower than the value of the initial feeding ANI/VC ratio, which indicates that only a part of the monomer polymerized and the product covered the VC surface during the *in situ* polymerization process. VC has a higher conductivity than PANI; however, when the PANI/VC ratio equals to 0.28 the global conductivity is further improved. This result can be explained by the fact that VC is porous and loose, thus the electrons find difficulty in transferring between particles. When VC surface is covered by a thin PANI serving as a binder, the VC particles can get combined all together resulting in a lower interface resistance, and thus, in a higher conductivity. On the other hand, the electronic donor-acceptor interactions between PANI and carbon can be resumed as a complex charge transfer, which results from the π-bond on the carbon surface interacting with PANI, which is conjugated π-bonded, especially to the quinoid ring.[20,32]

TABLE I
Effect of Feeding Ratio of ANI/VC on the Synthesized Product PANI/VC

ANI/VC feeding weight ratio	PANI/VC weight ratio	ANI polymerization Conv. (%)	Conductivity (S cm^{-1})
0	0	–	2.8
0.125	0.08	65.4	4.1
0.25	0.12	48.5	6.3
0.5	0.28	56.5	11
0.75	0.44	58.5	7.5
1	0.7	70.2	2.5
1.5	1.15	76.4	0.9
2	1.63	81.2	0.5
∞	∞	–	0.8

Figure 1 shows the FTIR spectra obtained for VC particles. The peak at 1600 cm^{-1} is related to aromatic rings, corresponding to the basic structural feature of carbon. The peak at 1230 cm^{-1} is attributed to the oxygen-containing group (—C—O—) on the carbon surface: its strength increases after pretreatment by HNO_3 and a carbonyl peak also appears at 1730 $cm^{-1.}$ More oxygen-containing groups (e.g., —OH and —COOH) will help improving carbon hydrophilia and surface wettability, resulting in better dispersion in aqueous solution. During the platinization process, it will also promote and uniform the absorption of the Pt precursor on the carbon surface, which is useful to form properly dispersed Pt particles.[33]

Figure 2 shows the morphology of VC particles (a) and PANI/VC composites (b, c) pretreated VC

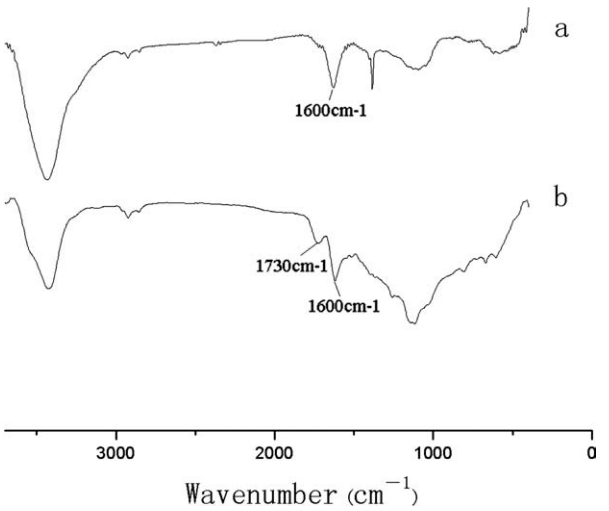

Figure 1 FTIR spectra of (a) untreated VC and (b) HNO_3 pretreated VC carbon powders.

particles disperse evenly. After VC compounded with PANI in a PANI/VC mass ratio of 0.28, polymer coat onto the carbon particles. When PANI/VC = 0.44, some additional tiny nanowires appear linked to the nanostructured PANI coating VC particles. From this evidence, we conclude that in low quantity of ANI, the VC particles were coated with PANI by *in situ* deposition of the formed conducting polymer, oligomer, or anilinium cations from the aqueous medium because of the electrostatic attraction of the carboxylic anion. But if the amount of ANI further increases, ANI may exist in form of anilinium cations or free aniline in the reaction solution. Furthermore, these two forms of ANI may self-assemble into micelle where the polymerization of aniline takes place. Zhang et al. stated that in the absence of a surfactant, micelles formed by anilinium cations could be considered as templates in the formation of the nanofiber.[34] And it has shown that with the polymerization of aniline proceeding the micelle consisting of anilinium cation and free aniline can change to rods through elongation.[35] Hence, it is reasonable to expect that the micelle would finally form PANI nanowires that deposited onto the core-shell structure of PANI/VC particles.

The peak at 1720 cm^{-1} corresponding to carboxylic group on VC particles [Fig. 3(a)] appears also on the spectra obtained for the PANI/VC composites [Fig. 3(b)], which differ from the spectrum of pure PANI [Fig. 3(c)]. The spectra of the composites exhibit clear benzoid (N—B—N) and quinoid (N=Q=N) ring skeleton vibrations of PANI macromolecules at 1470 and 1565 cm^{-1}, which can be seen at 1490 and 1588 cm^{-1} respectively in the case of pure PANI. The strong band at 1150 cm^{-1} was described by MacDiarmid as the "electronic-like band" and considered to be a measure of the degree of delocalization of electrons, thus, it is a characteristic peak associated to PANI conductivity.[36,37]

The FTIR spectra of the PANI/VC composites show several obvious differences in comparison with the spectrum of pure PANI. First of all, the spectra of the composites have a higher strength ratio of the previously described peaks (I_{quin}/I_{benz}) and a lower vibration frequency (Table II) with respect to the spectrum of pure PANI. The fact that the relative intensity of the electronic-like band (I_{e-l}/I_{quin}) in the composites is much higher than in the pure PANI, indicates that the composites have a higher conductivity than pure PANI. Please note that I_{e-l} is the intensity of the electronic-like band, whereas I_{quin} is the intensity of quinoid ring vibrations at 1565cm$^{-1.}$ During *in situ* polymerization, ANI monomers and the growing molecular chains, acting as electron-donors, will react with carbon, acting as electron-acceptor.[38] This interaction will increase PANI doping degree, leading to a higher conductivity. To some extent, in the final composite, VC particles will act as the doping agent for PANI macromolecules. It is well known that the imide group of quinine is the effective doping point. After doping, the electron cloud rearranges and part of the positive charge delocalizes towards the aromatic ring, resulting in a lower electronic density of the aromatic ring and in a consequently lower vibration frequency. When the PANI/VC ratio increases, the complex charge transfer helps these phenomena, increasing conductivity before PANI agglomeration. When PANI/VC ratio equals to 0.28, I_{e-l}/I_{quin} reaches its highest value, indicating that

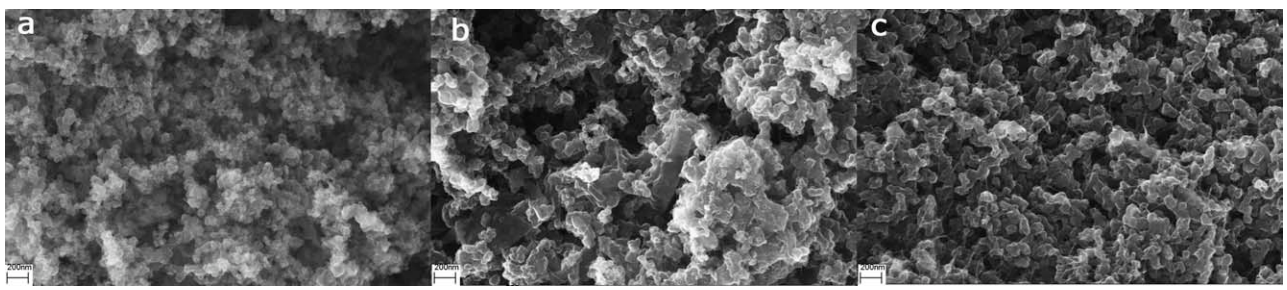

Figure 2 SEM micrographs of (a) pretreated VC, (b) PANI/VC (0.28), and (c) PANI/VC (0.44) composite.

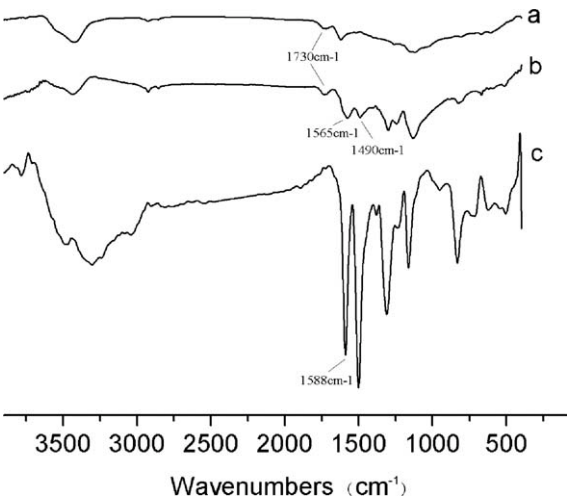

Figure 3 FTIR spectra of (a) pretreated VC, (b) PANI/VC (0.28), and (c) pure PANI.

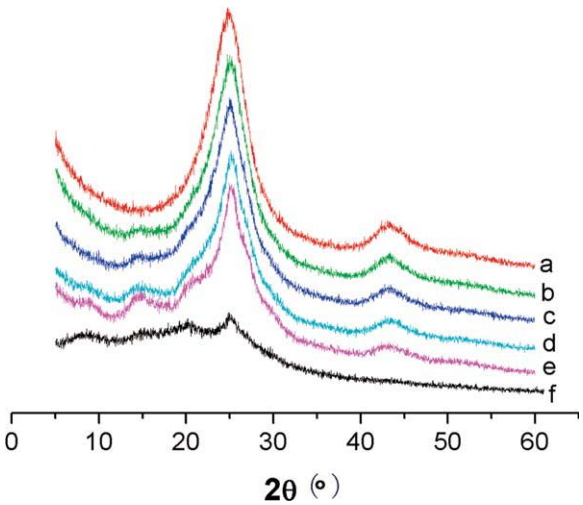

Figure 4 XRD spectra of PANI/VC supports (weight ratio): (a) 0, (b) 0.08, (c) 0.12, (d) 0.28, (e) 0.44, (f) ∞. [Color figure can be viewed in the online issue, which is available at www.interscience.wiley.com.]

conductivity is optimum. Too much PANI would cause agglomeration, which in turns, would lower conductivity and counteract with the charge transfer effect. As previously discussed, a PANI/VC ratio of 0.28 represents the critical point to assure that the charge transfer effect contributes to the amelioration of composite properties. Above such a critical point, PANI agglomerates contrast the benefits and result in a lower conductivity.

In this work, the reducing agent was used in excess with respect to the stoichiometric ratio to chloroplatinic acid, so that it is possible to assume that Pt feeding quantity can be seen as a loading quantity. Figure 4 shows the XRD patterns of different supports. For the VC particles (a), the diffraction peaks are observed at $2\theta = 26.2°$ and 42.5°, corresponding to C(002) and C(100) crystal faces.[39] For PANI macromolecules (*f*), the crystalline peaks appear at $2\theta = 8.8°$, 15.0°, 20.4°, and 24.9°, corresponding to (001), (011), (020), and (200) crystal planes in PANI emeraldine salt form.[40] The XRD data for the PANI/VC composites (b–e) reveal crystalline peaks including all the evidences already obtained for the pure PANI and VC particles. As the PANI content increases, more and more PANI macromolecules cover the surface of the VC particles, and the specific peaks of pure PANI become better visible, whereas the diffraction peaks corresponding to the carbon particles get weaker. Evidences show that a thin polymer layer effectively covers the surface of the carbon nanoparticles.

TABLE II
FTIR Analysis Results of PANI/VC Composites

Composite	I_{e-l}/I_{quin}	I_{quin}/I_{benz}
PANI/VC (0.08)	1.00	1.22
PANI/VC (0.12)	1.39	1.17
PANI/VC (0.28)	1.64	1.04
PANI/VC (0.44)	1.45	1.00
Pure PANI	0.75	0.87

The morphology and structure of catalysts

On the basis of SEM morphological characterizations, no substantial differences can be directly observed among the samples. Pt is a heavy element when compared with PANI components (C, N, H), thus it appears as a dark area in TEM images because of the atomic contrast. From TEM results, it can be seen (Fig. 5) that Pt clusters agglomerate to some extent and disperse on the surface of neat VC particles nonhomogeneously and sparsely. Pt clusters have a widely distributed and large particle sizes, which are about 10–70 nm. In contrast, there is a homogeneous dispersion of spherical Pt clusters on the exterior portion of PANI/VC composites (PANI/VC = 0.28). In this case, Pt clusters have a narrow size distribution, ranging from 4 to 7 nm. It can be seen that the VC support modified by PANI adsorption turns out to assist Pt in dispersing homogeneously.

Figure 6 shows the XRD spectra for platinized VC particles and PANI/VC composites (PANI/VC= 0.28). The peaks at 39.9°, 46.5°, 67.8°, 81.2°, 85.8° correspond to [111], [200], [220], [311], [222] crystal planes of Pt.[41] According to the measurement of the width of the strongest peak (Pt[111]) at half of its height the size of Pt grains can be calculated by the Scherrer formula[42]: $B(2\theta) = 0.94\lambda/L\cos\theta$. $B(2\theta)$ is half-peak width, λ is the incident wavelength

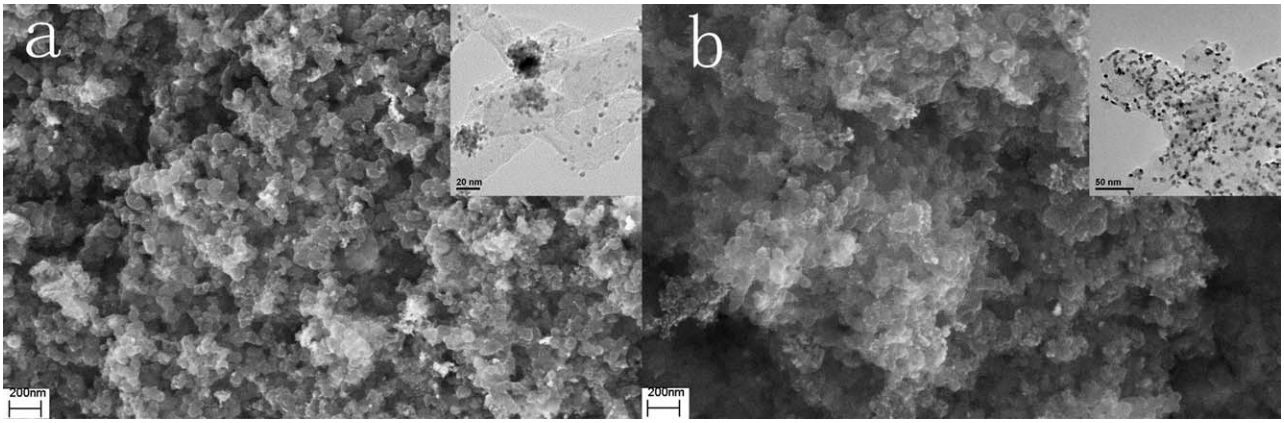

Figure 5 SEM and TEM micrograph of (a) Pt/VC and (b) Pt/PANI/VC catalyst (PANI/VC = 0.28 wt).

(0.1542 nm), L is the particle radius, and θ is the diffraction angle. On the composite supports, the calculated size is 4.5 nm, less than the value obtained on the carbon support (10.8 nm). The reduced size is favorable as it will provide a larger specific surface of the Pt particles, improving their catalysis efficiency.

The relative intensity of Pt(111) peak (i.e., $I_{Pt(111)}/I_0$) for the final Pt/PANI/VC composites gives a value (61.6), which is higher than the value obtained for Pt/VC systems (55.4). The value of I_0 is obtained as: $I_0 = I_{Pt(111)} + I_{Pt(200)} + I_{Pt(220)} + I_{Pt(311)} + I_{Pt(222)}$. In other words, it is shown here that there are more Pt(111) crystal faces available in Pt/PANI/VC composite catalyst with respect to the traditional Pt/VC catalyst. Indeed, Pt(111) is the active crystalline face having high antipoisoning ability,[43,44] therefore, the stability of the catalyst is also increased.

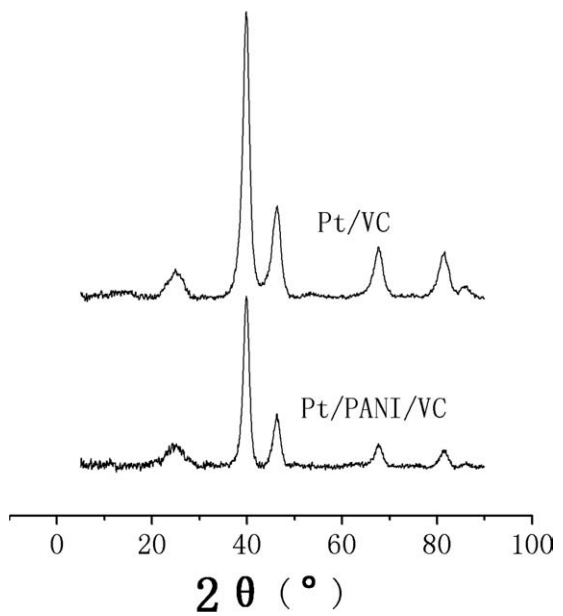

Figure 6 XRD pattern of Pt/VC and Pt/PANI/VC catalysts (PANI/VC = 0.28 wt).

The electrochemical activity of catalyst electrodes

Table III shows the peak current densities and potentials, as well as the onset oxidation potentials for the CV curves obtained for the platinized PANI/VC composite electrodes in a 1.0 mol/L methanol + 1.0 mol/L H_2SO_4 media. It is possible to observe that increasing the amount of VC particles in the composite will also increase methanol oxidized peak current, because carbon has a higher conductivity than PANI. When PANI/VC = 0.12 or 0.28, the peak potential and onset oxidation potential of the composites are the most negative. We conclude that their catalytic activities are better than others. However, some researchers reported that the electrodes containing Pt modified by pure conventional PANI made the redox reaction difficult to happen. O'Mullane,[22] for instance, reported that the onset peak of hydrazine oxidation on PANI/Pt is higher than the one for Pt wire electrode. On the other hand, Rajesh[26] reported that the use of a nanostructured conducting polymer as a support for Pt particles not only increases the electronic–ionic contact but also provides an easier electronic pathway in comparison with Pt deposited on carbon substrates. The activity of methanol oxidation is defended by several effects.

TABLE III
The data for Methanol Oxidation CV Curves of Platinized Different PANI/VC Composite

Catalyst	Peak current (mA/cm^2)	Peak potential (V)	Onset oxidation potential (V)
Pt/PANI/VC (0.08)	15.8	0.79	0.54
Pt/PANI/VC (0.12)	11.2	0.73	0.49
Pt/PANI/VC (0.28)	8.47	0.72	0.53
Pt/PANI/VC (0.44)	4.18	0.75	0.65

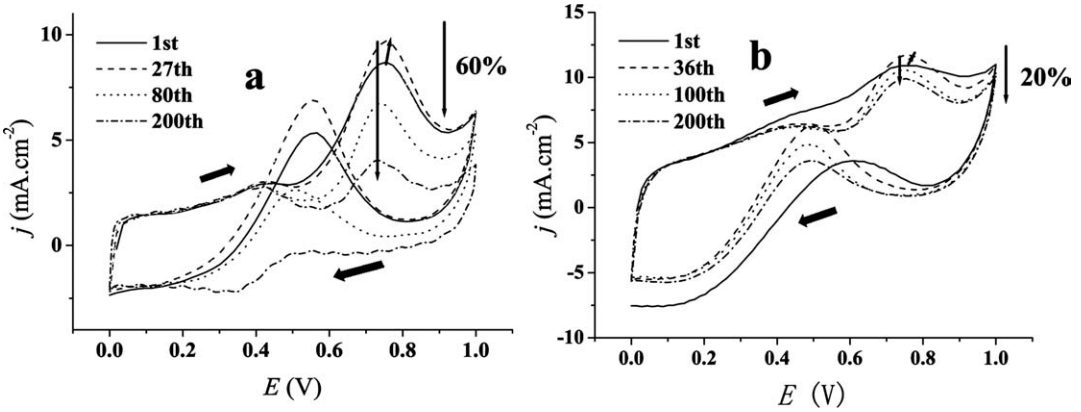

Figure 7 CV curves for (a) Pt/VC and (b) Pt/PANI/VC catalyst (PANI/VC = 0.28 wt) modified GC electrodes for 200 circles in 1.0 mol/L H_2SO_4 + 1.0 mol/L CH_3OH media.

In this case, nanostructured PANI/VC composite helps the process of methanol oxidation better than neat VC particles, as proved by the higher ratio I_{e-l}/I_{quin} measured by FTIR spectroscopy. The condition to be avoided is an excess of PANI (which is the case of pure PANI), as it leads to the formation of polymer agglomerates, thus, deteriorating the activity of methanol oxidation. The reason why a PANI/VC ratio equals to 0.12 or 0.28 is most effective depends on the two competitive factors.

Figure 7 shows the performances of the catalyst described so far for methanol oxidation by cyclic potential scan over 200 cycles. Two oxidative peaks located in 0.75 and 0.55 V are visible. It can be seen that the current reduces after having firstly increased (from the first cycle to the 27th cycle). At the end of 200 cycles, current decrease is 20% for Pt/PANI/VC (b) and 60% for Pt/VC (a). Therefore, the activity and stability of the Pt/PANI/VC electrode are higher in comparison with the values obtained for the Pt/VC electrode.

Even after more than 30 years of fundamental studies, the mechanism of methanol oxidation are not yet properly understood. The hypothesis of a bifunctional mechanism is likely to be more acceptable.[45–47] The reaction mechanism for methanol oxidation on Pt particles includes three stages, suggested as the following:

1. The absorption and activation of methanol on catalyst

$$CH_3OH_{aq} + Pt \longrightarrow Pt\text{—}CH_3OH_{ads} \quad (1)$$

$$Pt\text{—}CH_3OH_{ads} \longrightarrow Pt\text{—}CHO_{ads} + 3H^+ + 3e^- \quad (2)$$

$$Pt\text{—}CHO_{ads} \longrightarrow Pt\text{—}CO_{ads} + H^+ + e^- \quad (3)$$

2. The activation of molecular water on catalyst

$$Pt + H_2O \longrightarrow Pt\text{—}OH_{ads} + H^+ + e^- \quad (4)$$

3. The reaction between adsorbed species

$$Pt\text{—}CHO_{ads} + Pt\text{—}OH_{ads} \longrightarrow CO_2 + 2H^+ + 2e^- + 2Pt \quad (5)$$

$$Pt\text{—}CO_{ads} + Pt\text{—}OH_{ads} \longrightarrow CO_2 + H^+ + e^- + 2Pt \quad (6)$$

From the aforementioned description of the mechanism of methanol oxidation, it is clear that a modification of the coverage capability of the absorbed OH is vital to the improvement of the overall oxidation rate. The reasons why the activity of Pt/PANI/VC catalyst is higher may be the followings. First, the presence of PANI macromolecules actuates the adsorption of water so that active oxygen species ($Pt\text{—}OH_{ads}$) are generated, which urge the $Pt\text{—}CO_{ads}$ to turn into CO_2 desorbing away easilly. Second, PANI macromolecules in the composite support improve the dispersion of Pt particles (Fig. 4) and increase the amount of available Pt(111) crystalline faces (as confirmed by the XRD results), which in turns improves the antipoisoning ability, that is, increases the stability of the catalyst and decreases the adsorption sites for CO poisons.[48] Third, one could discuss about the possibility that some size effect influence the final results, aiming to the optimization of particle size and size distribution. This topic is actually largely controversial. Luna[49] supports this hypothesis and reports evidences to prove it. Contrarily, Watanabe[50] affords an example to prove hardly size effect. It is reasonable to think that an ideal diameter would make absorption and release facile in structure factor. As observed by

SEM and TEM characterizations, the diameter of Pt particles is obviously influenced by the support. The other key factor to the performances of Pt-dispersed catalyst is the uniformity of such dispersion. The CO_{ads} oxidation takes place only on the edges of the CO adsorbent islands.[51] At least four adjacent adsorption sites will be needed to strip all the hydrogen atoms of the methyl group in methanol.[52] Homogeneous dispersion of Pt catalysts on the PANI/VC support, which means better surface properties of the electrode, produces a higher activity in comparison with the one observed for the support without PANI. On the contrary, at a given loading percent, Pt agglomerates result less efficient without PANI, essentially because agglomeration affects surface properties (roughness and regularity). In the case, the size effect due to Pt particles, as well as, the other key parameters (dispersion) can not be ignored. A more homogeneous dispersion and a smaller size of the Pt particles certainly benefit to the electrochemical performances of the obtained catalyst. Fourth, the growth of a three-dimensional structure of microparticles supported by a polymeric film, instead of a two-dimensional layer of particles deposited on the bare electrode is another important advantage.[25] Fifth, higher electronic-like band, as discussed when evaluating FTIR spectra for the Pt/PANI/VC composite, makes it possible that Pt and PANI have some synergistic effect on methanol oxidation. Finally, the modified electrode containing PANI promotes CH_3OH and H_2O Langmuir adsorption, which also plays a promoting role.[53]

CONCLUSIONS

To improve the performances of Pt catalyst resisting CO poisoning, core/shell composites of PANI and VC were synthesized by *in situ* chemical polymerization. The platinized PANI/VC composite catalysts were prepared by chemical reduction method. The highest conductivity is obtained when the PANI/VC mass ratio equals to 0.28. And there are some reactions happened between PANI and VC, which are identified by FTIR. SEM, TEM, and XRD measurements indicated that the size of the Pt particles on the composite supports is smaller and their distribution is more uniform than on pure VC supports. Cyclic voltammetry measurements have shown that the attenuation degree of current of methanol oxidation after 200 cycles is only one-third of the value observed in the case of Pt/VC catalyst. It has been proved that the ability to resist CO poisoning and the consequent electrocatalysis stability of the composite catalyst increases. The composites are expected to be used as a support for Pt particles in methanol electrocatalytic oxidation.

References

1. Bagotzky, V. S.; Vassilyev, Y. B. Electrochim Acta 1967, 1323.
2. Léger, J. M. J Appl Electrochem 2001, 31, 767.
3. Prabhuram, J.; Zhao, T. S.; Liang, Z. X.; Chen, R. Electrochim Acta 2007, 52, 2649.
4. Du, H. D.; Li, B. H.; Kang, F. Y.; Fu, R. W.; Zeng, Y. Q. Carbon 2007, 45, 429.
5. Han, K.; Lee, J.; Kim, H. Electrochim Acta 2006, 52, 1697.
6. Zhang, X.; Zhang, F.; Chan, K. Y. J Mater Sci 2004, 39, 5845.
7. Umeda, M.; Ojima, H.; Mohamedi, M.; Uchida, I. J Power Sources 2004, 136, 10.
8. Chu, D.; Jiang, R. Z. Solid State Ionics 2002, 148, 591.
9. Bai, Y. X.; Li, J. F.; Qiu, X. P.; Wu, J. J.; Wang, J. S.; Xi, J. Y.; Zhu, W. T.; Chen, L. Q. J Mater Sci 2007, 42, 4508.
10. Saha, M. S.; Li, R. Y.; Sun, X. H. J Powder Source 2008, 177, 314.
11. Gu, Y. J.; Wong, W. T. Langmuir 2006, 22, 11447.
12. Wang, C.; Waje, M.; Wang, X.; Tang, J. M.; Haddon, R. C.; Yan, Y. Nano Lett 2004, 4, 345.
13. Bessel, C. A.; Laubernds, K.; Rodriguez, N. M.; Baker, R. T. J Phys Chem B 2001, 105, 1115.
14. Chang, H.; Joo, S. H.; Pak, C. J Mater Chem 2007, 17, 3078.
15. Chai, G. S.; Yoon, S. B.; Yu, J. S.; Choi, J. H.; Sung, Y. E. J Phys Chem B 2004, 108, 7074.
16. Fang, B.; Kim, J. H.; Lee, C.; Yu, J. S. J Phys Chem 2008, 112, 639.
17. Sevilla, M.; Lota, G.; Fuertes, A. B. J Power Sources 2007, 171, 546.
18. Blunk, R. H.; Abd Elhamid, M. H.; Lisi, D. J.; Mikhail, Y. M. U.S. Pat. 2003/096151 (2004).
19. Yoshii, Y.; Karasawa, H.; Higashiyama, K.; Iizuka, H.; Kanno, S.; Suzuki, S. U.S. Pat. 2003/096151 (2003).
20. Zengin, H.; Zhou, W.; Jin, J.; Czerw, R.; Smith, D. W., Jr.; Echegoyen, L.; Carroll, D. L.; Foulger, S. H.; Ballato, J. Adv Mater 2002, 14, 1480.
21. Rajesh, B.; Ravindranathan Thampi, K.; Bonard, J. M.; Mathieu, H. J.; Xanthopoulos, N.; Viswanathan, B. J Power Sources 2005, 141, 35.
22. O'mullane, A. P.; Dale, S. E.; Macpherson, J. V. Chem Commun 2004, 14, 1606.
23. Kessler, T.; Castro Luna, A. M. J Solid State Electrochem 2003, 7, 593.
24. Kinyanjui, J. M.; Wijeratne, N. R.; Hanks, J.; Hatchett, D. W. Electrochim Acta 2006, 51, 2825.
25. Golikand, A. N.; Golabi, S. M.; Maragheh, M. G.; Irannejad, L. J Power Sources 2005, 145, 116.
26. Rajesh, B.; Thampi, K. R.; Bonard, J. M.; Mcevoy, A. J.; Xanthopoulos, N.; Mathieu, H. J.; Viswanathan, B. J Power Sources 2004, 133, 155.
27. Wu, G.; Li, L.; Li, J. H.; Xu, B. Q. Carbon 2005, 43, 2579.
28. Choi, J. H.; Park, K. W.; Lee, H. K.; Kim, Y. M.; Lee, J. S.; Sung, Y. E. Electrochim Acta 2003, 48, 2781.
29. Souza, F. G., Jr.; Sirelli, L.; Michel, R. C.; Soares, B. G.; Herbst, M. H. J Appl Polym Sci 2006, 102, 535.
30. Karim, M. R.; Lee, C. J.; Lee, M. S. J Appl Polym Sci 2007, 103, 1973.
31. Jeevananda, T.; Siddaramaiah, T. S.; Lee, J. H.; Samir, O. M.; Somashekar, R. J Appl Polym Sci 2008, 109, 200.
32. Baibarac, M.; Baltog, I.; Lefrant, S.; Mevellec, J. Y.; Chauvet, O. Chem Mater 2003, 15, 4149.
33. Roman-Martinez, M. C.; Cazorla-Amoros, D.; Linares-Solano, A.; Salinas-Martinez De Lecea, C.; Yamashita, H.; Anpo, M. Carbon 1995, 33, 3.
34. Zhang, Z. M.; Wei, Z. X.; Wan, M. X. Macromolecules 2002, 35, 5937.
35. Harada, M.; Adachi, M. Adv Mater 2000, 12, 839.

36. Chen, R. J.; Zhang, Y.; Wang, D.; Dai, H. J Am Chem Soc 2001, 123, 3838.
37. Yu, Y. J.; Che, B.; Si, Z. H.; Li, L.; Chen, W.; Xue, G. Synth Met 2005, 150, 271.
38. Su, C.; Wang, G.; Huang, F. J Appl Polym Sci 2007, 106, 4241.
39. Zaragoza-Martín, F.; Sopeña-Escario, D.; Morallón, E.; De Lecea, C. S. M. J Power Sources 2007, 171, 302.
40. Pouget, J. P.; Jozefowicz, M. E.; Epstein, A. J.; Tang, X.; Macdiarmid, A. G. Macromolecules 1991, 24, 779.
41. Do, J. S.; Chen, Y. T.; Lee, M. H. J Power Sources 2007, 172, 623.
42. Alauzun, J.; Mehdi, A.; Reyé, C.; Corriu, R. Chem Mater 2007, 19, 6373.
43. Jarvi, T. D.; Sriramulu, S.; Stuve, E. M. Colloids Surf A 1998, 134, 145.
44. Spendelow, J. S.; Xu, Q.; Goodpaster, J. D. J Electrochem Soc 2007, 154, 238.
45. Vigier, F.; Gloaguen, F.; Leger, J.-M.; Lamy, C. Electrochim Acta 2001, 46, 4331.
46. Niu, L.; Li, Q. H.; Wei, F. H.; Wu, S. X.; Liu, P. P.; Cao, X. L. J Electroanal Chem 2005, 578, 331.
47. Gojkovic, S. L.; Vidakovic, T. R. Electrochim Acta 2001, 47, 633.
48. Napporn, W. T.; Laborde, H.; Leger, J. M.; Lamy, C. J Electroanal Chem 1996, 404, 153.
49. Luna, A. M. C. J Appl Electrochem 2000, 30, 1137.
50. Watanabe, M.; Saegusa, S.; Stonehart, P. J Electroanal Chem 1989, 271, 213.
51. Roth, J. D.; Weaver, M. J. J Electroanal Chem 1990, 307, 119.
52. Munk, J.; Christensen, P. A.; Hamnett, A.; Skou, E. J Electroanal Chem 1996, 401, 215.
53. Rajendra Prasad, K.; Munichandraiah, N. J Power Sources 2002, 103, 300.